The Company of **Biologists**

RESEARCH ARTICLE

Quiescent center initiation in the *Arabidopsis* lateral root primordia is dependent on the *SCARECROW* transcription factor

Tatsuaki Goh[1,2,*,‡], Koichi Toyokura[1], Darren M. Wells[2], Kamal Swarup[2], Mayuko Yamamoto[1], Tetsuro Mimura[1], Dolf Weijers[3], Hidehiro Fukaki[1], Laurent Laplaze[4], Malcolm J. Bennett[2] and Soazig Guyomarc'h[5,‡]

ABSTRACT

Lateral root formation is an important determinant of root system architecture. In *Arabidopsis*, lateral roots originate from pericycle cells, which undergo a program of morphogenesis to generate a new lateral root meristem. Despite its importance for root meristem organization, the onset of quiescent center (QC) formation during lateral root morphogenesis remains unclear. Here, we used live 3D confocal imaging to monitor cell organization and identity acquisition during lateral root development. Our dynamic observations revealed an early morphogenesis phase and a late meristem formation phase as proposed in the bi-phasic growth model. Establishment of lateral root QCs coincided with this developmental phase transition. QC precursor cells originated from the outer layer of stage II lateral root primordia, within which the *SCARECROW* (*SCR*) transcription factor was specifically expressed. Disrupting SCR function abolished periclinal divisions in this lateral root primordia cell layer and perturbed the formation of QC precursor cells. We conclude that *de novo* QC establishment in lateral root primordia operates via SCR-mediated formative cell division and coincides with the developmental phase transition.

KEY WORDS: Lateral root organogenesis, Quiescent center, *SCARECROW*, 3D live imaging, *Arabidopsis thaliana*

INTRODUCTION

The plasticity of plant root system architecture provided by post-embryonic lateral root (LR) formation greatly contributes to its adaptability to environmental conditions (Bao et al., 2014). LRs facilitate nutrient and water acquisition by increasing soil exploration. While primary root initiation, organization and growth have been extensively studied, the molecular and cellular mechanisms that control the patterning of new lateral root primordia (LRPs) are still poorly characterized (Tian et al., 2014a). Root growth results from the activity of the root apical meristem (RAM), a group of proliferating cells organized around a central stem cell

niche (SCN). The RAM of the primary root (PR) is created during early embryogenesis through formative cell divisions and initial cell identity is maintained by an organizing center termed the quiescent center (QC) (Perilli et al., 2012; ten Hove et al., 2015). A number of regulatory mechanisms have been identified that control QC establishment and maintenance in the PR, especially in the model plant *Arabidopsis thaliana*. The phytohormone auxin controls the specification of the hypophysis (the QC precursor cell) during embryogenesis and later maintains QC function in seedling roots with the AP2-domain *PLETHORA* (*PLT*) transcription factors (Moller and Weijers, 2009; ten Hove et al., 2015). The maintenance of the QC and SCN during post-embryonic primary root growth relies on the activity of *PLT* and GRAS-family transcription factors *SHORT-ROOT* (*SHR*) and *SCARECROW* (*SCR*) in combination with an auxin gradient (Bennett and Scheres, 2010; Perilli et al., 2012).

Despite similarities between primary and lateral root meristems, these structures are generated in different tissue and genetic contexts, and many of the processes governing the generation of a new root meristem in LRP remains to be elucidated (Lavenus et al., 2013; Tian et al., 2014a). In particular, little is known about the patterning processes controlling *de novo* establishment of the QC and SCN in the developing LRP (Laskowski et al., 1995; Tian et al., 2014a). In *A. thaliana*, LRs originate from a subset of approximately six pericycle cells that divide and form a new root apical meristem with a radially symmetrical structure akin to the PR (Lavenus et al., 2013). A pioneering study of *Arabidopsis* lateral root development by Ian Sussex and co-workers originally proposed that LR organogenesis occurs in two successive steps: first, an early morphogenesis phase during which a primordium composed of three to five layers of approximately isodiametric cells is generated; second, a meristem formation phase, during which cell identity patterning and meristem organization occurs, generating the characteristic tissue structure of the root apex (Laskowski et al., 1995). Later, Malamy and Benfey (1997) performed an extensive analysis of LRP morphogenesis and proposed eight developmental stages (stage I to stage VII and emergence) based on anatomical criteria and these structural milestones have been confirmed in later studies (Lucas et al., 2013; von Wangenheim et al., 2016). In summary, LRP formation is initiated when asymmetric anticlinal cell divisions of founder cells produce pairs of abutting small cells flanked by longer cells (stage I; Goh et al., 2012). Next, the central smaller cells undergo three further rounds of periclinal cell divisions to create a four-layered primordium (stages II to IV). During stages V and VI, the LRP acquires a cellular organization similar to the primary RAM. At the emergence stage, the LRP finally breaks through overlying root tissues and enters the soil (Lavenus et al., 2013; Malamy and Benfey, 1997). Thus, an anatomical organization reminiscent of a presumptive organizing center was first observed in longitudinal sections of stage VI lateral root

[1]Department of Biology, Graduate School of Science, Kobe University, Kobe 657-8501, Japan. [2]Centre for Plant Integrative Biology, School of Biosciences, University of Nottingham, Nottingham LE12 5RD, UK. [3]Laboratory of Biochemistry, Wageningen University, 6703 HA Wageningen, The Netherlands. [4]Institut de Recherche pour le Développement, Unité Mixte de Recherche (UMR) Diversité Adaptation et Développement des plantes (DIADE), Montpellier 34394 Cedex 5, France. [5]Université de Montpellier, Unité Mixte de Recherche (UMR) Diversité Adaptation et Développement des plantes (DIADE), Montpellier 34394 Cedex 5, France.
*Present address: Graduate School of Biological Sciences, Nara Institute of Science and Technology, 8916-5 Takayama, Ikoma, Nara 630-0192, Japan.

‡Authors for correspondence (goh@bs.naist.jp; soazig.guyomarch@ird.fr)

T.G., 0000-0002-1064-5801

Received 15 January 2016; Accepted 26 July 2016

DEVELOPMENT

primordia. However, the dynamics of QC establishment during LRP development has remained elusive (Tian et al., 2014a).

Here, we investigated further the classical two-step LRP developmental model formulated by Sussex and co-workers (Laskowski et al., 1995), focusing on the mechanisms controlling *de novo* QC formation during LRP development. We developed a 3D time-lapse confocal laser-scanning microscopy imaging approach to analyze development of living lateral root primordia. We observed that QC formation, as reported by QC marker gene expression, occurs at the transition between the early morphogenesis phase and the later meristem organization phase of LRP development. These two events also coincide with a 3D organ shape change from bilateral to radial. Cell lineage analysis revealed that the QC originates from the outer layer of stage II LRP. We report that the GRAS family transcription factor *SCR* regulates QC formation by controlling formative periclinal cell divisions that give rise to QC precursor cells. We conclude that *de novo* QC establishment in LR depends on *SCR* expression in the outer layer of stage II primordia and coincides with a developmental phase transition.

RESULTS

LR formation exhibits a bi-phasic pattern of growth

To understand the molecular and cellular mechanisms controlling LR organogenesis, a confocal laser scanning microscopy (CLSM)-based 3D time-lapse imaging approach was developed using a transgenic line ubiquitously expressing a plasma membrane-localized yellow fluorescent protein (YFP)-tagged reporter termed WAVE131Y (Geldner et al., 2009). Images were taken at 10 min intervals as *z*-stacks (2 µm step) over a 24 h period. This strategy allowed us to observe the entire process of LRP morphogenesis spanning early developmental stages up to organ emergence at high temporal and spatial resolution and was compatible with the monitoring of live functional cell markers. Precise analysis of a

time-lapse 3D image series of developing LRP obtained using this method was consistent with the 2D anatomical stages described by Malamy and Benfey (1997). Importantly, our imaging technique also allowed us to explore the kinetics of LRP morphogenesis throughout these stages (Fig. 1A,B and Movie 1). Following anticlinal divisions of founder cells creating a one-layered stage I primordium, later periclinal divisions generate a two-layered LRP (stage II; Fig. 1A, *t*=0:00), which subsequently undergoes new anticlinal divisions to produce a stage II primordium composed of small cells (Fig. 1A, *t*=4:00, white arrowheads). A second round of periclinal cell divisions in the outer layer of stage II (Fig. 1A, *t*=7:00, white arrowhead) then creates a three-layered primordium (termed stage III). A third round of periclinal divisions (this time in the innermost cell layer) produces a four-layered LRP (termed stage IV; Fig. 1A, *t*=9:30, white arrowhead). In summary, during this early morphogenesis phase (stages I to IV), well-coordinated anticlinal and periclinal cell divisions generate a four-layered LRP. Stage V was characterized by anticlinal divisions at the flanking cells of outer layers (Fig. 1A, *t*=14:00, arrowheads) and elongation of inner cells (Fig. 1A, *t*=14:00 and 15:00, denoted by two-directional arrows). Stage VI LRP exhibited periclinal and anticlinal cell divisions that produced the endodermal and cortical layers, and periclinal cell divisions in the outermost layer that will give rise to the root cap (Fig. 1A, *t*=21:00, arrowheads; Fig. S1). Thus, through characteristic cell divisions and cell elongation events in stage V and VI, an anatomically recognizable meristematic structure is formed as early as stage VI, consistent with results initially described by Malamy and Benfey (1997).

During the early LRP morphogenesis phase (stages I to IV), cell divisions remained constrained within the space between underlying protoxylem and overlying endodermal tissues (Fig. 1A,B). Both protoxylem and endodermal cells contain lignified walls (termed the Casparian strip in the latter case) that provide these tissues with structural rigidity (Naseer et al., 2012).
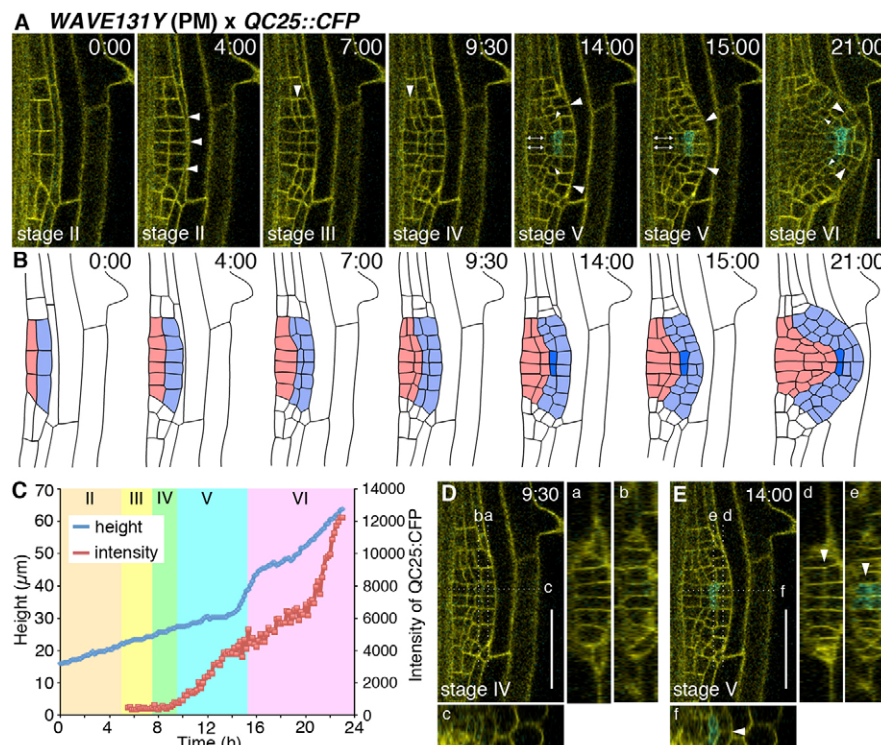
Fig. 1. Cellular patterning and QC establishment during *Arabidopsis* LR primordium development. (A) Time-lapse image series of LR primordium development visualized using WAVE131Y (plasma membrane, yellow) and QC25::CFP (QC marker, cyan). White arrowheads and two-directional arrows indicate the characteristic cell divisions and cell elongation, respectively. The elapsed time (h:min) after the start of observation and developmental stage are indicated on each panel. See also Movie 1. Scale bar: 50 µm. (B) Cell lineage map of the LRP shown in A. The inner and outer layers of stage II (*t*=0:00) are shown in light blue and pink, respectively. The cells derived from each layer are indicated by the same color. Dark blue indicates outer layer-derived cells that showed a QC25::CFP signal. (C) Quantification of LRP height (blue) and QC25::CFP fluorescence intensity (red). QC25::CFP intensity was quantified at the center cells of the second outermost layer. LRP developmental stages are categorized according to a previous paper (Malamy and Benfey, 1997). (D,E) Front view (a,b,d and e) and top-down view (c and f) of digitally sliced images of A [*t*=9:30 (D) and 14:00 (E)]. The white dotted lines in the side view images indicate the positions of the sliced planes. White arrowheads indicate the longitudinal radial cell divisions at the outermost (d) or second outermost layer (e) of the stage V LRP (E, *t*=14:00). Scale bars: 50 µm.

DEVELOPMENT

These rigid cell walls, especially the Casparian strip, provide mechanical constraints on LRPs, which impact the LRP morphogenesis (Lucas et al., 2013; Vermeer et al., 2014). Consistent with this, our time-lapse image data revealed that the rate of organ outgrowth (inferred from changes in its height) remained slow until stage V (Fig. 1C), and LRP shape was flattened when the LRP was passing through the endodermal layer (Fig. 1A, t=7:00, 9:30 and 14:00). Then, the growth rate of LRP significantly accelerated (Fig. 1C) and LRP changed to dome-shaped from the end of stage V (meristem formation phase; Fig. 1A, t=15:00) (Kumpf et al., 2013; Lucas et al., 2013). This expansion of the LRP seems principally caused by axial elongation of cells at the base of the primordium (depicted by two-directional arrows in Fig. 1A, t=14:00 and 15:00).

Taken together, these time-lapse observations of developing primordia suggested that LRP formation operates in two developmental phases: an early morphogenesis phase (stages I to IV) during which a four-layered LRP is formed, constrained between the xylem pole and the endodermis, and a later meristem formation phase (stage V onwards) characterized by the onset of a mature meristem structure and rapid organ outgrowth. This is consistent with the hypothesis that LRP formation is a bi-phasic growth process as originally proposed by Laskowski et al. (1995), with phase transition occurring at stage V as described by Malamy and Benfey (1997).

3D cell division orientation and LRP shape change coincides with a developmental phase transition

We previously reported that LRPs initially exhibit bilateral symmetry that later changes to radial symmetry, adopting a cylindrical shape similar to the PR (Lucas et al., 2013). Tangential divisions at the flanking side contribute to the 3D LRP shape change by creating a ring of cells surrounding the central dividing cells (Lucas et al., 2013). In order to better understand the contribution of division plane orientation to the 3D LRP shape and its relationship with the LRP developmental phase transition, we monitored nuclear dynamics by employing our time-lapse imaging

system with the nuclear-localized reporter line *pRPS5a::H2B: tdTomato* (Adachi et al., 2011) and then tracked LRP nuclei movement and cell divisions (Fig. 2A-F, Fig. S2). This 4D tracking of nuclei showed the contributions of daughter cells derived from pericycle cell files adjacent to the xylem pole in the 3D LRP structure and revealed that LRPs are predominantly formed from cells in three files of pericycle cells (Fig. 2A-F, Movie 2). Consistent with previous analysis (Kurup et al., 2005; von Wangenheim et al., 2016), the central pericycle file provided all of the cells in the central median plane (green), whilst cells derived from adjacent pericycle files (red and orange) contributed to the LRP flanks (Fig. 2A-F, Movie 2). Until stage IV, cells from the central cell file underwent three rounds of periclinal cell division to create a four-layered primordium (t=12:00, Fig. 2A,B). Around the phase transition (stage V, t=16:00, Fig. 2C,D, Movie 2), an abrupt reorientation of the cell division plane (termed longitudinal) occurred in the median file of the LRP, contributing to primordium widening (t=22:00, Fig. 2E,F, white arrows). Careful analysis of cell division patterns in WAVE131Y-expressing LRP revealed that new longitudinal planes of cell divisions indeed promoted LRP widening at stage V (Fig. 1E, tangential sections d and e, arrowheads). Hence, cell division plane re-orientation at stage V contributes to 3D LRP shape change towards a cylindrical structure, concomitant with the early-to-late LRP morphogenesis phase transition. Thus, a developmental transition takes place at stage V during LRP development, and encompasses two events: the change from an early four-layer primordium generation phase to a later meristem organization phase, and a switch from bilateral to radial organ growth.

QC formation occurs simultaneously with an LRP developmental transition at stage V

In the PR, QC cells function as an organizing center regulating the activity and maintenance of the stem cell niche (SCN; Bennett and Scheres, 2010; Perilli et al., 2012). Despite its fundamental importance for meristem formation and subsequent growth of new LRs, nothing is known about the spatio-temporal regulation of post-embryonic formation of QC cells. To address this, we initially
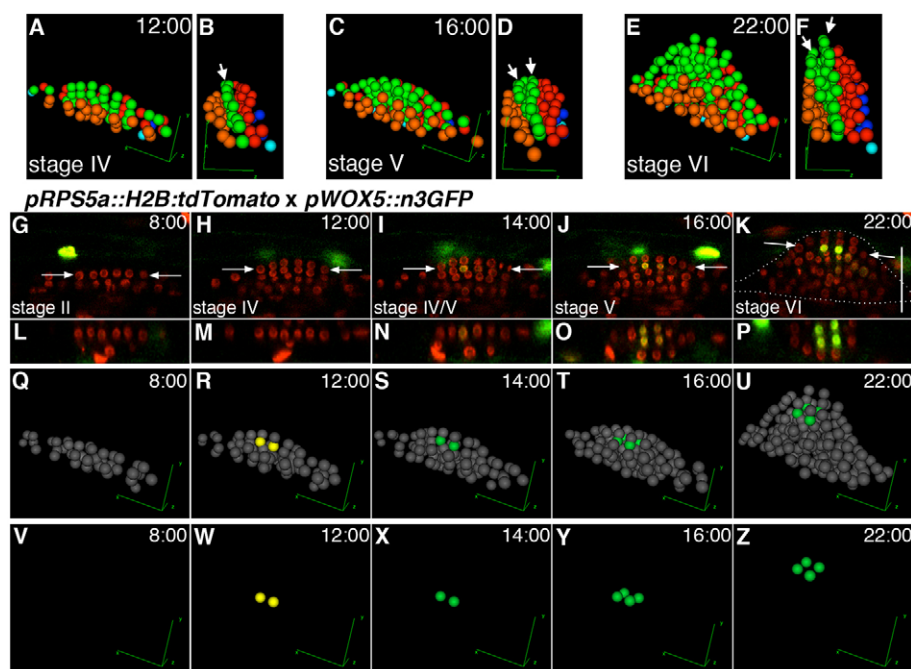
Fig. 2. 4D nuclear tracking analysis of LRP development. (A-F) The contributions of each pericycle cell file to LRP development visualized by 3D nuclei representation. Nuclei movement and division in the time-lapse data shown in G-K were tracked and are represented using 3D spheres. A,C and E are side views of the LRP; and B,D and F are top-down views. The central cell file of stage I and its lineage are indicated in green; and flanking cell lineages are indicated in orange and red. Blue and light blue indicate additional flanking cell files of stage I. White arrows indicate the central cell file with longitudinal radial cell division at stage V. See also Movie 2. (G-K) Time-lapse image series of LRP development visualized using *pRPS5a::H2B: tdTomato* (red) and *pWOX5::n3GFP* (green). The elapsed time (h:min) from the start of observation and developmental stage are indicated on each panel. See also Movie 3. Scale bar: 50 μm. (L-P) Front views of digitally sliced images at the indicated positions (white arrows) of G-K. (Q-U) 3D nuclei representation of the QC lineage in the LRP. The QC precursor cell (before *WOX5* expression, yellow) and *WOX5*-positive QC (green) are shown with the surrounding lineage (gray). See also Movie 4. (V-Z) 3D nuclei representation of only the QC lineage from Q-U.

studied the expression dynamics of the QC-specific reporter line *QC25::CFP* (ten Hove et al., 2010) using our time-lapse imaging system. *QC25::CFP* expression was first detected in cells at the center of the second outermost layer at stage IV/V, and the reporter signal was enhanced at a later stage (Fig. 1A-E, Movie 1). The expression of *QC25::CFP* was initiated before the characteristic cell divisions and accelerated organ outgrowth at the later meristem formation phase (Fig. 1A,C, Movie 1).

To confirm this observation and explore how QC formation is related to 3D structural changes of the LRP, we performed nuclear tracking in developing primordia expressing both *pWOX5::n3GFP* and *pRPS5a::H2B:tdTomato* markers (Fig. 2G-Z, Movie 3). The second QC marker *pWOX5::n3GFP* exhibited an identical spatial and temporal expression pattern to *QC25::CFP* in the LRP (Fig. 1 and Fig. 2G-K; Movies 1 and 3), initially being detected in the central cells of the second outermost layer of stage IV/V just prior to phase transition (*t*=14:00, Fig. 2I,N,S,X). Importantly, the longitudinal divisions occurred simultaneously with expression of *WOX5* (Fig. 2J,O,T,Y, Movie 4) and *QC25::CFP* (Fig. 1E). Digital cross-sections revealed that the expression of both QC reporters was detected in a subset of four LRP cells located in the center of the second outermost layer of stage V primordia (Fig. 1E, tangential section e; Fig. 2O,P,T,U,Y,Z; Movie 4), suggesting that the central single cell file produced a group of four QC cells by reorientation of the cell division plane (i.e. longitudinally) at stage V. Based on the timing of induction of both *QC25* and *WOX5* markers, we conclude that QC establishment coincides with the developmental transition from an initial basic cellular organization with bilateral symmetry to the later meristem formation phase with progressive acquisition of radial symmetry.

QC cells originate from the outer layer of stage II LRP

To help determine how the QC is established during the earlier stages of development, we tracked cell lineages in developing LRP using our time-lapse series of CLSM images (Fig. 1B). Our analysis revealed that vascular and pericycle tissues originated from the inner layer of stage II LRP (indicated in pink in Fig. 1B), whereas the outer layer of stage II LRP gave rise to the epidermis, ground tissues (endodermis and cortex) and root cap tissues (shown in light blue in Fig. 1B; Fig. S1). Our dynamic cell-fate analysis validated the lineage model proposed by Malamy and Benfey (1997). In addition, our analysis revealed that QC cells are derived from the outer layer of stage II LRP. More precisely, the central daughter cells of the second outermost layer, after the second periclinal division of the outer layer of stage II LRP, were specified as QC precursor cells, in which the expression of QC markers was initiated at stage V (Fig. 1A,B; QC cells are shown in dark blue in Fig. 1B). Hence, the differentiation of inner and outer layers in the stage II LRP appears to be an important event preceding QC specification and subsequent root meristem patterning.

SHR and SCR expression domains distinguish inner and outer LRP layers

Earlier studies have reported that the GRAS-type transcription factor *SCARECROW* (*SCR*) is one of the earliest genes exhibiting differential LRP expression, specifically in the outer layer of stage II primordia (Malamy and Benfey, 1997). *SCR* interacts with another GRAS-type transcription factor, *SHORT-ROOT* (*SHR*), to regulate SCN maintenance, ground tissue formation and organ growth in the PR (Fisher and Sozzani, 2016). Using our time-lapse imaging system, a functional *pSCR::GFP:SCR* marker [in a *scr-3* mutant background (Gallagher et al., 2004)] was first detected in stage II

LRP specifically in the outer layer (Fig. 3A, *t*=4:00 and 8:00; Fig. 3F; Movie 5). Following periclinal division of the outer layer of stage II LRP, the GFP:SCR protein was initially detected in both daughter cell layers (Fig. 3A, *t*=12:00; Fig. 3G), but the signal gradually disappeared from the outermost layer (Fig. 3A, *t*=16:00), while it was maintained in the nuclei of cells within the second outermost layer of the LRP after stage III (Fig. 3A, *t*=20:00; Fig. 3H). The second outermost layer-specific expression of the *SCR* gene was confirmed using a transcriptional *pSCR:GUS:GFP* reporter (Fig. 3C-E). Consistent with previous reports (Malamy and Benfey, 1997; Tian et al., 2014b), our dynamic live confocal observations revealed how the *SCR* expression domain forms during LRP development.

SCR transcription is largely dependent on *SHR* (Helariutta et al., 2000; Levesque et al., 2006). In primary RAMs, the *SHR* gene is expressed in stele cells (including the pericycle), where the SHR protein is localized in the cytosol and nucleus, but the SHR protein moves via plasmodesmata to nuclei of adjacent QC and endodermal cells, where it activates *SCR* expression (Nakajima et al., 2001). In stage I LRP, the functional SHR:GFP protein expressed under the control of its own regulatory region (*pSHR::SHR:GFP*) in the *shr-2* mutant background (Nakajima et al., 2001) was detected very weakly in all cells (Fig. 3B, Movies 6 and 7, *t*=0:00). In stage II LRP, the SHR:GFP protein signal gradually increased in cells of the inner layer while it was weakly detected in the outer layer (Fig. 3B, *t*=4:00 and 8:00), where the SHR:GFP proteins locate in the nucleus (Fig. 3B,L). From stage III onwards, the SHR:GFP protein signal remained high in the inner layer-derived tiers, and gradually increased in the nuclei of cells of the second outermost layer directly overlying *SHR*-expressing inner layer-derived cells (Fig. 3B, *t*=12:00-20:00, M,N, Movies 6 and 7). The inner layer-specific expression of the *SHR* gene was confirmed using a transcriptional *pSHR:GUS* reporter (Fig. 3I-K), consistent with published results (Lucas et al., 2011). The appearance of SHR:GFP protein in cell nuclei in the second outermost layer of the LRP coincided with an enhanced level of GFP:SCR signal in those cells (Fig. 3A,B), consistent with *SCR* transcription being largely SHR dependent (Helariutta et al., 2000; Levesque et al., 2006). Thus, our imaging system helped refine our knowledge of *SCR* and *SHR* expression dynamics in developing primordia and revealed that in stage II LRP, the SHR and SCR transcriptional domains delineate the inner and outer cell layers, respectively, which might be functionally important for further primordium morphogenesis.

The *scr* mutation disrupts QC establishment

To determine the functional importance of *SCR* outer layer-specific expression in stage II primordia, we analyzed LRP morphogenesis in the *scr-3* mutant using time-lapse imaging (Figs 4 and 5). In wild-type plants, periclinal divisions in stage II LRPs occurred according to a regular sequence: cells divided initially in the outer layer, and subsequently in the inner layer (Fig. 1A, *t*=7:00 and 9:30; Movie 1). After stage II periclinal division, two or three rounds of cell divisions were observed in the outermost layer-derived cells over the following 20 h (Fig. 5A, blue box and nuclei; Fig. S3). Slower divisions were observed in the cells derived from the second outermost layer of stage IV in the same time period (Fig. 5A, red box and nuclei; Fig. S3). In contrast, cell divisions in the outer layer of the *scr-3* mutant LRPs were largely abolished during early primordia development (Fig. 4A,B, *t*=6:00; Movie 8), while the inner layer underwent periclinal divisions. Later, cell divisions in the outer layer-derived tiers of the primordium occurred only once in a small number of central cells during the 20 h of our time-lapse
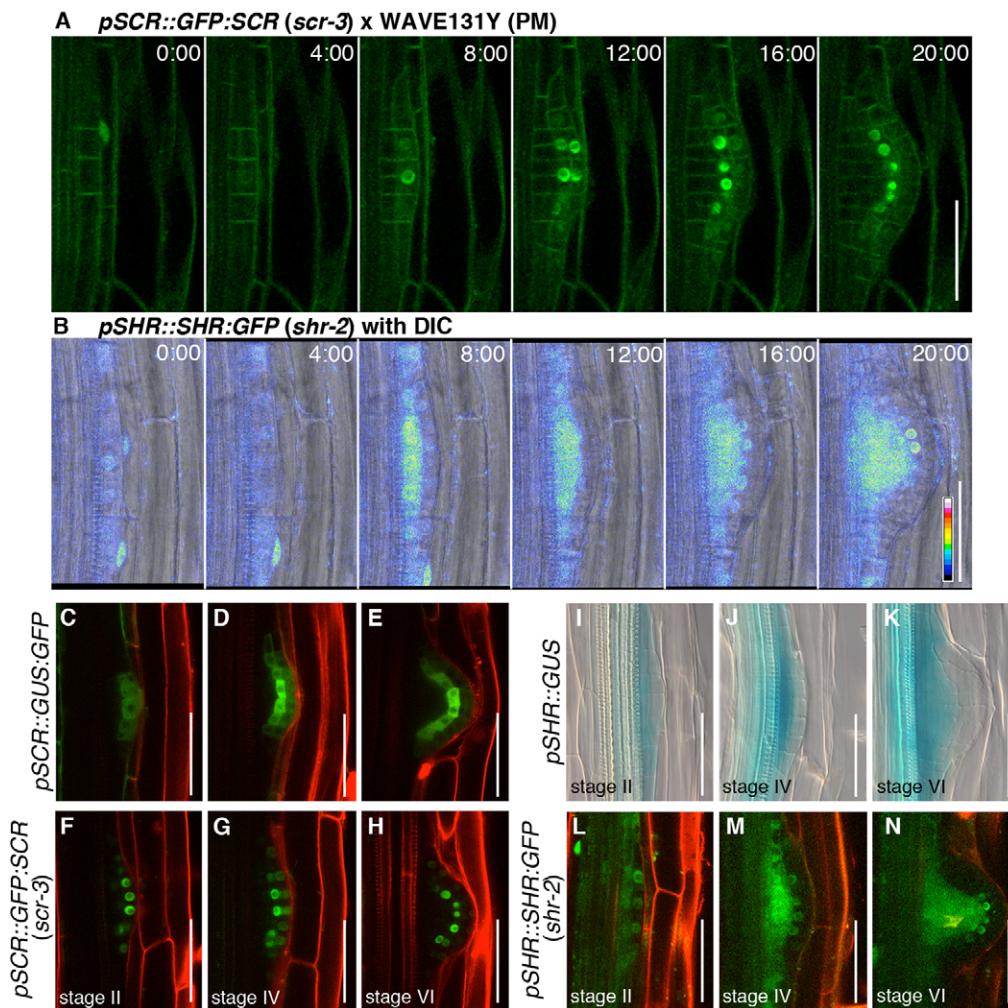
Fig. 3. SCR and SHR expression domains delineate the inner and outer LRP layers. (A) Time-lapse image series of *pSCR::GFP:SCR (scr-3)*×WAVE131Y (plasma membrane) initiated from the stage I LRP. GFP::SCR is localized in the nuclei. The elapsed time (h:min) from the start of observation is indicated in each panel. See also Movie 5. (B) Time-lapse image series of *pSHR:: SHR:GFP (shr-2)* merged with DIC starting from stage I. The fluorescence intensity of SHR:GFP is described by a rainbow look-up color table. The elapsed time (h:min) from the start of observation is indicated in each panel. See also Movies 6 and 7. (C-E) Expression pattern of *SCR* transcriptional reporter (*pSCR::GUS: GFP*) at stage II (C), IV (D) and VI (E). (F-H) Expression pattern of *SCR* translational reporter (*pSCR::GFP: SCR scr-3*) at stage II (F), IV (G) and VI (H). (I-K) Expression pattern of *SHR* transcriptional reporter (*pSHR:GUS*) at stage II (I), IV (J) and VI (K). (L-N) Expression pattern of *SHR* translational reporter (*pSHR::SHR: GFP shr-2*) at stage II (L), IV (M) and VI (N). Scale bars: 50 μm.

observation, although inner layer-derived cells continued to divide in a wild-type fashion (Fig. 4A,B, *t*=11:30 and 18:00; Fig. 5B; Fig. S3; Movie 8). As a consequence, after stage II, it is difficult to assign precise stages to developing *scr-3* primordia according to Malamy and Benfey's nomenclature. Hence, *SCR* appears to promote the second round of periclinal cell divisions in the outer layer of stage II LRP, as well as subsequent divisions of the outer layer derivatives, whereas inner layer cell divisions are independent of SCR function.

In order to confirm the specific cell division defects in the outer layer of the *scr-3* mutant, we monitored the spatial activity of the *SCR* promoter (*pSCR::GUS:GFP*) during LRP development. Whilst *pSCR:GUS:GFP* signal was clearly enhanced in the second outermost layer of wild-type LRPs at stage V (Fig. 4C,D), it appeared more uniform in *scr-3* cells derived from presumptive derivatives of the stage II outermost layer at approximately the same stage (Fig. 4E,F). We also observed similar defects in the periclinal cell division in the outer layer and spatial pattern of *SCR* promoter activity in *shr-2* (Fig. S4), consistent with the mutant's previously reported severe LRP patterning defects (Lucas et al., 2011). These observations suggested that defects in periclinal divisions in the stage II outermost layer of *scr-3* and *shr-2* LRP disrupt the correct spatial regulation of *SCR* expression during later LRP development. Based on these data, we conclude that periclinal divisions in the outer layer of stage II LRP (some of which generated the future QC cells) are regulated by *SCR* and *SHR*.

Our earlier cell lineage analysis revealed that the periclinal divisions in the outer layer of the stage II LRP are important for producing QC precursor cells (Fig. 1A,B). Thus, disrupting periclinal cell division in the outer layer of the *scr-3* stage II LRP would compromise QC formation. Indeed, nuclear expression of the *pWOX5::n3GFP* QC marker was undetectable in the *scr-3* mutant LRP prior to organ emergence (Fig. 6). At 24 h, WOX5 promoter activity was weakly detected at a QC-like position, after which reporter expression was strongly detected at later time points (Fig. 6). This observation suggested that specific expression of *SCR* in the outer layer of stage II promotes formative periclinal cell divisions to produce QC precursor cells and subsequent QC establishment in the LRP.

Nevertheless, *scr-3* LRP continued to develop as a result of the division of cells derived from the inner layer, and eventually, cells occupying similar positions to wild-type QC cells in *scr-3* LR expressed the *pWOX5::n3GFP* marker, albeit considerably later than the wild type (Fig. 6, *t*=28:30 and 34:00, red arrowheads). Consistent with this observation, the *scr* mutant created mature LRs, although they were shorter than those in the wild type (Fig. S5), possibly because of later defects in SCN maintenance by similar mechanisms to the PR (Sabatini et al., 2003). Interestingly, tracking the origin of the QC marker-positive cells in the *scr-3* mutant revealed that they were derived from inner layer cells of the stage II LRP (Fig. 6B, shown in pink). Our observations suggest that QC formation in the LRP is normally dependent on *SCR*-mediated
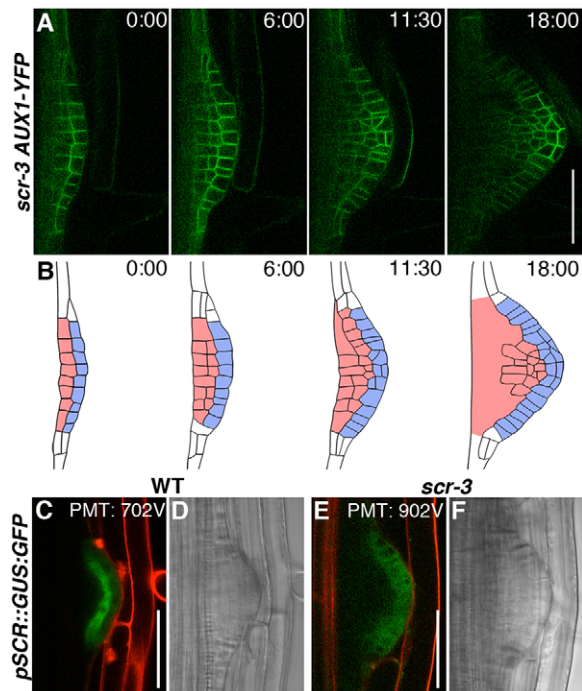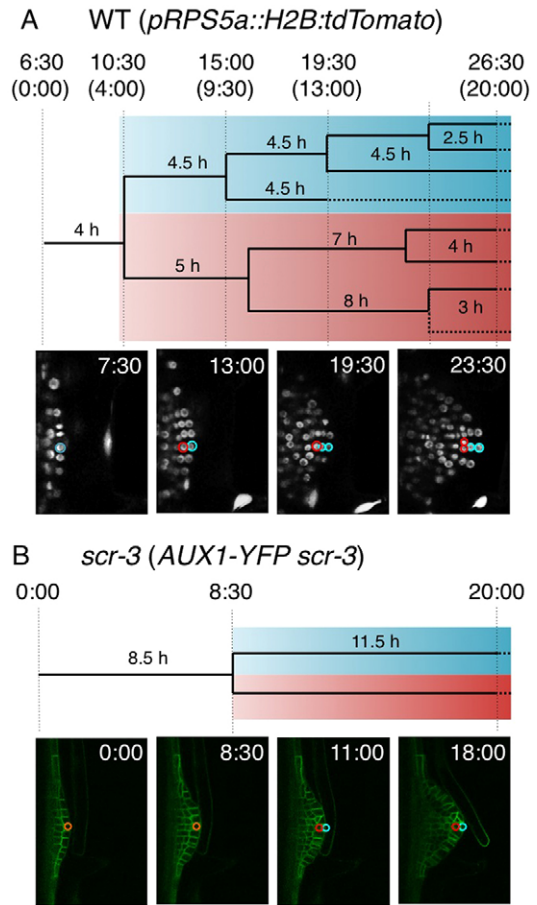
Fig. 4. SCR promotes periclinal cell divisions in the outer layer of stage II LRP. (A) Time-lapse image series of LRP development in *AUX1-YFP scr-3*. *AUX1-YFP* was used as a plasma membrane marker (green). The elapsed time (h:min) from the start of observation is indicated in each panel. See also Movie 8. (B) Cell lineage map of the LRP shown in A. The inner and outer layers of stage II (*t*=0:00) are shown in light blue and pink, respectively. Cells derived from the same layer are indicated by the same color. (C-F) *SCR* promoter activity in the wild type and *scr-3* mutant. *pSCR::GUS:GFP* was observed in the second outermost layer of the wild type (C,D) and the outermost layer of the *scr-3* mutant (E,F). Because of the large reduction of *SCR* promoter activity in the *scr-3* mutant compared with the wild type, we observed expression using different voltages on a photo multiplier (PMT); 702 V for the wild type and 902 V for *scr-3* with the same laser power (5%). The roots are counterstained with propidium iodide (red). Scale bars: 50 µm.


Fig. 5. Cell divisions in the outer layer-derived tiers are largely abolished in the *scr-3* mutant. (A) Cell lineage tree of the central cell at the outer layer of stage II LRP of the wild type. Cell divisions of the target cell-derived lineage from stage II (*t*=6:00) were traced in the *pRPS5a::H2B:tdTomato* time-lapse data (Fig. 2) for 20 h. (B) Cell lineage tree of the central cell in the outer layer of stage II LRP of *scr-3* (*AUX1-YFP scr-3*, Fig. 4). Only one cell division was observed in the cell lineage over 20 h from stage II. Branch lengths indicated approximate time for cell cycle analyzed by 30 min intervals. Dotted branches indicate the cells out of observed stack.

periclinal cell division in the outer layer of the stage II LRP. However, when the normal pattern of QC establishment is defective, QC cells still eventually establish, albeit independent of SCR regulation via a distinct LRP cell lineage.

DISCUSSION

LR formation represents a highly integrated and dynamic process that transforms LR founder cells into new root meristems. Here, we describe *de novo* establishment of QC and meristem organization during LRP morphogenesis. A 3D time-lapse confocal imaging approach revealed that LRP development operates in a bi-phasic manner: first, from stages I to IV, periclinal and anticlinal cell divisions create a simple four-layered primordium with respect to the main growth axes of pericycle cells. From stage V onwards, more-complex cell division patterning contributes to meristem formation accompanied with accelerated growth and 3D shape change to a radially cylindrical structure similar to the PR. Our time-lapse analyses of live LRP development are consistent with previously reported results (Laskowski et al., 1995; Malamy and Benfey, 1997) and further support the model of a biphasic morphogenesis process initially proposed by Laskowski et al. (1995) (Fig. 7).

Our confocal-based time-lapse imaging system allowed us to analyze live lateral root development with high spatio-temporal resolution. This approach is complementary to the light sheet fluorescent microscopy (LSFM)-based imaging technique reported by von Wangenheim and co-workers (2016). Both techniques enable 4D monitoring of living lateral root primordia. While LSFM offers 4D visualization of the root sample with reduced exposure to laser sources, our confocal-based approach provides advantages such as high resolution and flexible control of multi-colored imaging, by enabling visualization of multiple reporters simultaneously.

Our study also revealed that the transition between the two major phases of LRP development, namely early morphogenesis phase and late meristem formation phase, occurs in stage V primordia and coincides with the onset of QC marker gene expression in central cells of the second outermost layer. Despite previously reported observations suggesting earlier onset of *WOX5* expression during LR development (Ditengou et al., 2008), our repeated analyses of two new QC markers (*pWOX5::n3GFP* and *QC25::CFP*) support the conclusion that QC identity is established around stage V during LRP development.

Our study also reveals that QC establishment in LRs relies on the differentiation of the inner and outer layers in stage II primordia
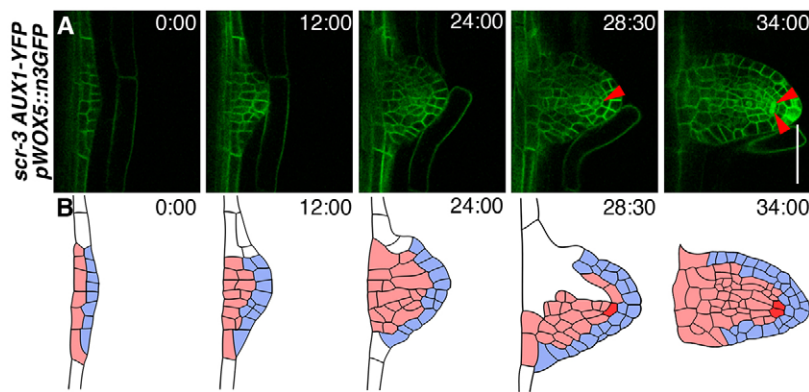
Fig. 6. The *scr* mutation disrupts the normal pattern of QC establishment in LRP. (A) Time-lapse image series of LRP development in *pWOX5::n3GFP AUX1-YFP* in the *scr-3* background. A nuclear signal indicates *pWOX5::n3GFP* expression (indicated by red arrowheads). The elapsed time (h:min) from the start of observation is indicated in each panel. Scale bar: 50 μm. (B) Cell lineage map of the LRP shown in A. The inner and outer layers of stage II (*t*=0:00) are colored light blue and pink, respectively. Red indicates inner layer-derived cells that have a *pWOX5::n3GFP* signal.

controlled by two GRAS-family transcription factors, *SCR* (outer layer) and *SHR* (inner layer). It is plausible that, as observed in the primary root meristem, SHR protein movement from the presumptive stele of stage II primordium to the overlying cell layer induces *SCR* expression and that SCR-SHR interaction later restricts *SCR* expression domain to the second outermost layer of the developing LRP (Cui et al., 2007). However, the precise mechanisms regulating *SHR* expression, migration and transcriptional activity in the context of lateral root development remain to be elucidated.

The *SCR*-expressing outer LRP layer produces QC precursor cells via *SCR*-regulated periclinal cell divisions. These observations are reminiscent of two functional properties of SCN regulation in the PR. First, *WOX5* expression in the PR meristem was shown to depend on the SCR/SHR regulation pathway (Sarkar et al., 2007). Thus, despite the differences in the tissue context of both events, regulation of *WOX5* expression by the SHR/SCR module seems to be conserved between primary and lateral root meristem formation. Second, earlier work on the PR has shown that *SHR* and *SCR* regulate formative cell divisions in root ground tissue initial cells, generating endodermal and cortical layers (Cruz-Ramirez et al., 2012; Sozzani et al., 2010). In this study, we report that in stage II LR primordia, SCR also regulates the formative periclinal division of the outer layer, preceding QC specification. This suggests that cell division pattern for QC establishment is regulated differently during LR development and embryogenesis in *Arabidopsis* (Wysocka-Diller et al., 2000) and that, while SCR is not strictly required for LR

QC establishment, 'normal' QC-forming formative divisions in the lateral root primordium depend on SCR function.

Ian Sussex and co-workers originally proposed that the formation of a LR meristem is a two-step process (Laskowski et al., 1995) and hypothesized that there is an unknown developmental transition event between these two phases. We report that QC formation correlates with the transition from an early morphogenesis phase to a later meristem formation phase at stage V and with bilateral to radial 3D organ shape change. Before that stage, the SCR/SHR module controls the initial inner/outer patterning of stage II primordium and promotes the formative periclinal cell division of the outer layer that precedes QC formation. After that stage, QC specification might contribute to orchestrate further steps of root meristem organization in the developing primordium. Primary root QC cells organize SCN activity and maintenance by controlling phytohormone distribution and the spatio-temporal activity of transcription factors (Perilli et al., 2012; ten Hove et al., 2015). It will be interesting to analyze how QC establishment influences meristem organization and maintenance in the second phase of LRP development, and to compare it with the regulatory networks operating in the primary root apex. Interestingly, despite being severely impaired in outer layer-derived cell divisions during the earlier developmental phase, ultimately, the *scr* mutant could still establish a QC at a similar position to that in the wild type. This observation suggests that cells in the early LRP of the *scr* mutant still have competency for QC establishment, which might have similar regulatory mechanisms to root regeneration (Sena et al., 2009; Xu et al., 2006). This emphasizes the robustness of LR
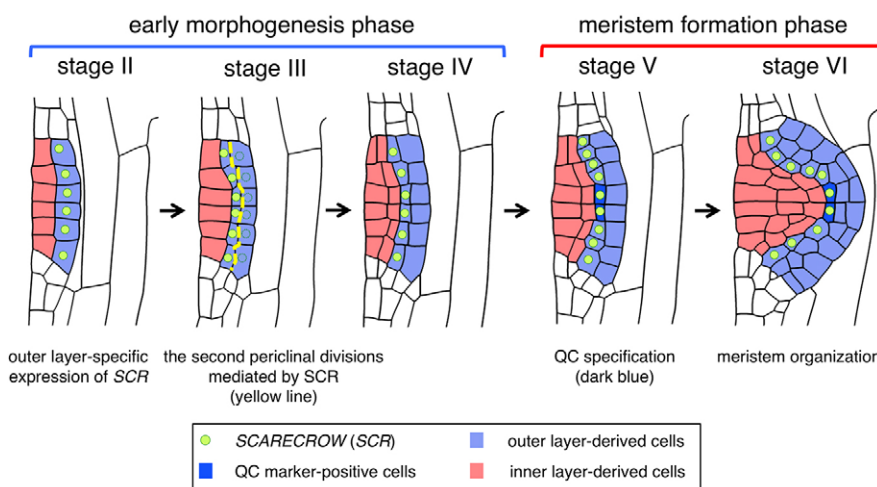
Fig. 7. Schematic model of *Arabidopsis* LR organogenesis. LR development is biphasic with an initial morphogenesis phase to form basic four-layered LRP followed by meristem formation phase as initially proposed by Laskowski et al. (1995). The transition from bilateral to radial 3D organ shape also coincides with the transition from early morphogenesis to late meristem formation phases. The GRAS-family transcription factor, *SCARECROW* (*SCR*) is specifically expressed in the outer layer of stage II and regulates the formation of precursor cells of QC through *SCR*-mediated periclinal cell divisions (indicated by yellow dashed line at stage III). QC establishment occurs simultaneously with and facilitates the developmental phase transition of LRP at stage V.

meristem patterning mechanisms with respect to cell lineage. We hypothesize that QC cell specification in the LR is regulated by yet to be determined positional information (e.g. phytohormones, mobile signals) and a dynamic gene regulatory network (Lavenus et al., 2015; Voss et al., 2015). Further analyses will help to address the SCR-independent patterning mechanisms for *de novo* QC specification in the LRP and shed light on the functional importance of this new stem cell niche for LRP development.

MATERIALS AND METHODS

Plant materials and growth conditions

The *A. thaliana* accession Col-0 was used throughout the experiments. The following transgenic plants were used: *QC25::CFP* (ten Hove et al., 2010), *WAVE131Y* (Geldner et al., 2009), *pRPS5a::H2B:tdTomato* (Adachi et al., 2011), *pSCR::GFP:SCR* (*scr-3*) (Gallagher et al., 2004), *pSHR::SHR:GFP* (*shr-2*) (Nakajima et al., 2001), *pSHR::GUS* (Helariutta et al., 2000), *shr-2* and *scr-3* (Fukaki et al., 1998) and *AUX1-YFP* (Swarup et al., 2004). Seeds were germinated under sterile conditions on 1× Murashige–Skoog medium solidified with 0.5% gellan gum containing 0.5 g/l MES-KOH (pH 5.8), 0.01% myo-inositol and 1% sucrose. Plants were grown at 23°C under continuous light in vertically orientated Petri dishes.

Vector construction and plant transformation

To generate *pSCR::GUS:GFP*, In-Fusion Cloning (TaKaRa) was used to clone a *SCR* promoter fragment (2349 bp) amplified by PCR with the primers pGWB-XbaI-AtSCRpro-F (GCAGGTCGACTCTAGAGACCGG-AGAGAGACCGGAGAA) and pGWB-XbaI-AtSCRpro-R (TGTTGAT-AACTCTAGAGTTGGTCGTGAGATTGCATGGT) into pGWB550 (Nakagawa et al., 2007). A *GUS* fragment amplified by PCR with the primers attB1-F-GUS (aaaaagcaggctCCATGGTCCGTCCTGTAGAAAC) and attB2-R-GUS (agaaagctgggtATTGTTTGCCTCCCTGCTGCG) was cloned into pDONR221 and transferred into pGWB550-AtSCRpro by the Gateway technology (Life Technology). To generate *pWOX5::n3GFP*, a ~4.6 kb fragment of the upstream region of *WOX5* was amplified as described previously (Sarkar et al., 2007) and then cloned upstream of SV40-3×GFP in pGreenIIKAN (Takada and Jurgens, 2007). The plasmid was introduced into Col-0 by the floral dip transformation method (Clough and Bent, 1998).

Time-lapse imaging of LR morphogenesis

For time-lapse imaging, 5-day-old plants were placed horizontally into a cover-glass-bottom chamber (Thermo Fisher Scientific) with a block of solid medium and observed under an inverted confocal microscope [Leica SP5II or Olympus FV1000 with a Z focus drift compensating system (ZDC)]. In order to allow plant growth on the microscope stage during image acquisition, a LED lighting system was coupled to the microscope hardware. On the Leica SP5II, an USB relay controller (KMtronic) and countdown timer software custom-written in the LabVIEW development environment (National Instruments) turned off the light during laser scanning. For the Olympus FV1000, a ring-shaped LED lamp attached to the microscope condenser was controlled by the TTL signal output from the FV1000. Images were taken every 10 or 15 min at 2 μm z-steps using a 60× water immersion objective lens with Immersol W 2010 (Zeiss) immersion medium and then processed with the ImageJ program Fiji (Schindelin et al., 2012) and its plugin Correct 3D drift (http://fiji.sc/Correct_3D_drift) for the registration of 3D+T image dataset. Each observation was repeated at least three times. For the cell lineage map, confocal images were traced using CellSet software (Pound et al., 2012) and then drawn in Illustrator (Adobe). The divisions and movements of nuclei labelled with *pRPS5a::H2B:tdTomato* (Adachi et al., 2011) were tracked with TrackMate (v.2.7.4) using Fiji (http://fiji.sc/TrackMate).

GFP observation and GUS staining

For GFP observation with a confocal microscope (Olympus FV1000), roots were counterstained with propidium iodide (PI, 10 μg/ml). For GUS staining, roots were prefixed with ice-cold 90% acetone for 15 min, and then stained with GUS staining solution [100 mM sodium phosphate, pH 7.0, 10 mM

EDTA, 5 mM potassium ferrocyanide, 5 mM potassium ferricyanide, 0.1% Triton X-100 and 0.5 mg/ml 5-bromo-4-chloro-3-indolyl-β-D-glucuronide (X-Gluc)]. Whole-mount clearing preparation of roots was performed using chloral hydrate. Samples were observed with a Leica DM6000 microscope equipped with Nomarski optics (Leica Microsystems).

References

Adachi, S., Minamisawa, K., Okushima, Y., Inagaki, S., Yoshiyama, K., Kondou, Y., Kaminuma, E., Kawashima, M., Toyoda, T., Matsui, M. et al. (2011). Programmed induction of endoreduplication by DNA double-strand breaks in *Arabidopsis. Proc. Natl. Acad. Sci. USA* **108**, 10004-10009.

Bao, Y., Aggarwal, P., Robbins, N. E., Sturrock, C. J., Thompson, M. C., Tan, H. Q., Tham, C., Duan, L., Rodriguez, P. L., Vernoux, T. et al. (2014). Plant roots use a patterning mechanism to position lateral root branches toward available water. *Proc. Natl. Acad. Sci. USA* **111**, 9319-9324.

Bennett, T. and Scheres, B. (2010). Root development-two meristems for the price of one? *Curr. Top. Dev. Biol.* **91**, 67-102.

Clough, S. J. and Bent, A. F. (1998). Floral dip: a simplified method for *Agrobacterium*-mediated transformation of *Arabidopsis thaliana*. *Plant J.* **16**, 735-743.

Cruz-Ramirez, A., Diaz-Trivino, S., Blilou, I., Grieneisen, V. A., Sozzani, R., Zamioudis, C., Miskolczi, P., Nieuwland, J., Benjamins, R., Dhonukshe, P. et al. (2012). A bistable circuit involving SCARECROW-RETINOBLASTOMA integrates cues to inform asymmetric stem cell division. *Cell* **150**, 1002-1015.

Cui, H., Levesque, M. P., Vernoux, T., Jung, J. W., Paquette, A. J., Gallagher, K. L., Wang, J. Y., Blilou, I., Scheres, B. and Benfey, P. N. (2007). An evolutionarily conserved mechanism delimiting SHR movement defines a single layer of endodermis in plants. *Science* **316**, 421-425.

Ditengou, F. A., Teale, W. D., Kochersperger, P., Flittner, K. A., Kneuper, I., van der Graaff, E., Nziengui, H., Pinosa, F., Li, X., Nitschke, R. et al. (2008). Mechanical induction of lateral root initiation in Arabidopsis thaliana. *Proc. Natl. Acad. Sci. USA* **105**, 18818-18823.

Fisher, A. P. and Sozzani, R. (2016). Uncovering the networks involved in stem cell maintenance and asymmetric cell division in the *Arabidopsis* root. *Curr. Opin. Plant Biol.* **29**, 38-43.

Fukaki, H., Wysocka-Diller, J., Kato, T., Fujisawa, H., Benfey, P. N. and Tasaka, M. (1998). Genetic evidence that the endodermis is essential for shoot gravitropism in *Arabidopsis thaliana*. *Plant J.* **14**, 425-430.

Gallagher, K. L., Paquette, A. J., Nakajima, K. and Benfey, P. N. (2004). Mechanisms regulating SHORT-ROOT intercellular movement. *Curr. Biol.* **14**, 1847-1851.

Geldner, N., Denervaud-Tendon, V., Hyman, D. L., Mayer, U., Stierhof, Y.-D. and Chory, J. (2009). Rapid, combinatorial analysis of membrane compartments in intact plants with a multicolor marker set. *Plant J.* **59**, 169-178.

Goh, T., Joi, S., Mimura, T. and Fukaki, H. (2012). The establishment of asymmetry in *Arabidopsis* lateral root founder cells is regulated by LBD16/ASL18 and related LBD/ASL proteins. *Development* **139**, 883-893.

Helariutta, Y., Fukaki, H., Wysocka-Diller, J., Nakajima, K., Jung, J., Sena, G., Hauser, M.-T. and Benfey, P. N. (2000). The *SHORT-ROOT* gene controls radial patterning of the *Arabidopsis* root through radial signaling. *Cell* **101**, 555-567.

Kumpf, R. P., Shi, C.-L., Larrieu, A., Sto, I. M., Butenko, M. A., Peret, B., Riiser, E. S., Bennett, M. J. and Aalen, R. B. (2013). Floral organ abscission peptide IDA and its HAE/HSL2 receptors control cell separation during lateral root emergence. *Proc. Natl. Acad. Sci. USA* **110**, 5235-5240.

Kurup, S., Runions, J., Köhler, U., Laplaze, L., Hodge, S. and Haseloff, J. (2005). Marking cell lineages in living tissues. *Plant J.* **42**, 444-453.

Laskowski, M. J., Williams, M. E., Nusbaum, H. C. and Sussex, I. M. (1995). Formation of lateral root meristems is a two-stage process. *Development* **121**, 3303-3310.

Lavenus, J., Goh, T., Roberts, I., Guyomarc'h, S., Lucas, M., De Smet, I., Fukaki, H., Beeckman, T., Bennett, M. and Laplaze, L. (2013). Lateral root development in *Arabidopsis*: fifty shades of auxin. *Trends Plant Sci.* **18**, 450-458.

Lavenus, J., Goh, T., Guyomarc'h, S., Hill, K., Lucas, M., Voss, U., Kenobi, K., Wilson, M. H., Farcot, E., Hagen, G. et al. (2015). Inference of the Arabidopsis lateral root gene regulatory network suggests a bifurcation mechanism that defines primordia flanking and central zones. *Plant Cell* **27**, 1368-1388.

Levesque, M. P., Vernoux, T., Busch, W., Cui, H., Wang, J. Y., Blilou, I., Hassan, H., Nakajima, K., Matsumoto, N., Lohmann, J. U. et al. (2006). Whole-genome analysis of the SHORT-ROOT developmental pathway in *Arabidopsis*. *PLoS Biol.* **4**, e143.

Lucas, M., Swarup, R., Paponov, I. A., Swarup, K., Casimiro, I., Lake, D., Peret, B., Zappala, S., Mairhofer, S., Whitworth, M. et al. (2011). Short-Root regulates primary, lateral, and adventitious root development in Arabidopsis. *Plant Physiol.* **155**, 384-398.

Lucas, M., Kenobi, K., von Wangenheim, D., Voss, U., Swarup, K., De Smet, I., Van Damme, D., Lawrence, T., Peret, B., Moscardi, E. et al. (2013). Lateral root morphogenesis is dependent on the mechanical properties of the overlaying tissues. *Proc. Natl. Acad. Sci. USA* **110**, 5229-5234.

Malamy, J. E. and Benfey, P. N. (1997). Organization and cell differentiation in lateral roots of *Arabidopsis thaliana*. *Development* **124**, 33-44.

Moller, B. and Weijers, D. (2009). Auxin control of embryo patterning. *Cold Spring Harb. Perspect. Biol.* **1**, a001545.

Nakagawa, T., Suzuki, T., Murata, S., Nakamura, S., Hino, T., Maeo, K., Tabata, R., Kawai, T., Tanaka, K., Niwa, Y. et al. (2007). Improved Gateway binary vectors: high-performance vectors for creation of fusion constructs in transgenic analysis of plants. *Biosci. Biotechnol. Biochem.* **71**, 2095-2100.

Nakajima, K., Sena, G., Nawy, T. and Benfey, P. N. (2001). Intercellular movement of the putative transcription factor SHR in root patterning. *Nature* **413**, 307-311.

Naseer, S., Lee, Y., Lapierre, C., Franke, R., Nawrath, C. and Geldner, N. (2012). Casparian strip diffusion barrier in Arabidopsis is made of a lignin polymer without suberin. *Proc. Natl. Acad. Sci. USA* **109**, 10101-10106.

Perilli, S., Di Mambro, R. and Sabatini, S. (2012). Growth and development of the root apical meristem. *Curr. Opin. Plant Biol.* **15**, 17-23.

Pound, M. P., French, A. P., Wells, D. M., Bennett, M. J. and Pridmore, T. P. (2012). CellSeT: novel software to extract and analyze structured networks of plant cells from confocal images. *Plant Cell* **24**, 1353-1361.

Sabatini, S., Heidstra, R., Wildwater, M. and Scheres, B. (2003). SCARECROW is involved in positioning the stem cell niche in the *Arabidopsis* root meristem. *Genes Dev.* **17**, 354-358.

Sarkar, A. K., Luijten, M., Miyashima, S., Lenhard, M., Hashimoto, T., Nakajima, K., Scheres, B., Heidstra, R. and Laux, T. (2007). Conserved factors regulate signalling in *Arabidopsis thaliana* shoot and root stem cell organizers. *Nature* **446**, 811-814.

Schindelin, J., Arganda-Carreras, I., Frise, E., Kaynig, V., Longair, M., Pietzsch, T., Preibisch, S., Rueden, C., Saalfeld, S., Schmid, B. et al. (2012). Fiji: an open-source platform for biological-image analysis. *Nat. Methods* **9**, 676-682.

Sena, G., Wang, X., Liu, H.-Y., Hofhuis, H. and Birnbaum, K. D. (2009). Organ regeneration does not require a functional stem cell niche in plants. *Nature* **457**, 1150-1153.

Sozzani, R., Cui, H., Moreno-Risueno, M. A., Busch, W., Van Norman, J. M., Vernoux, T., Brady, S. M., Dewitte, W., Murray, J. A. H. and Benfey, P. N. (2010). Spatiotemporal regulation of cell-cycle genes by SHORTROOT links patterning and growth. *Nature* **466**, 128-132.

Swarup, R., Kargul, J., Marchant, A., Zadik, D., Rahman, A., Mills, R., Yemm, A., May, S., Williams, L., Millner, P. et al. (2004). Structure-function analysis of the presumptive Arabidopsis auxin permease AUX1. *Plant Cell* **16**, 3069-3083.

Takada, S. and Jurgens, G. (2007). Transcriptional regulation of epidermal cell fate in the *Arabidopsis* embryo. *Development* **134**, 1141-1150.

ten Hove, C. A., Willemsen, V., de Vries, W. J., van Dijken, A., Scheres, B. and Heidstra, R. (2010). *SCHIZORIZA* encodes a nuclear factor regulating asymmetry of stem cell divisions in the *Arabidopsis* root. *Curr. Biol.* **20**, 452-457.

ten Hove, C. A., Lu, K.-J. and Weijers, D. (2015). Building a plant: cell fate specification in the early *Arabidopsis* embryo. *Development* **142**, 420-430.

Tian, H., De Smet, I. and Ding, Z. (2014a). Shaping a root system: regulating lateral versus primary root growth. *Trends Plant Sci.* **19**, 426-431.

Tian, H., Jia, Y., Niu, T., Yu, Q. and Ding, Z. (2014b). The key players of the primary root growth and development also function in lateral roots in Arabidopsis. *Plant Cell Rep.* **33**, 745-753.

Vermeer, J. E. M., von Wangenheim, D., Barberon, M., Lee, Y., Stelzer, E. H. K., Maizel, A. and Geldner, N. (2014). A spatial accommodation by neighboring cells is required for organ initiation in *Arabidopsis*. *Science* **343**, 178-183.

von Wangenheim, D., Fangerau, J., Schmitz, A., Smith, R. S., Leitte, H., Stelzer, E. H. K. and Maizel, A. (2016). Rules and Self-Organizing Properties of Post-embryonic Plant Organ Cell Division Patterns. *Curr. Biol.* **26**, 439-449.

Voss, U., Wilson, M. H., Kenobi, K., Gould, P. D., Robertson, F. C., Peer, W. A., Lucas, M., Swarup, K., Casimiro, I., Holman, T. J. et al. (2015). The circadian clock rephases during lateral root organ initiation in *Arabidopsis thaliana. Nat. Commun.* **6**, 7641.

Wysocka-Diller, J. W., Helariutta, Y., Fukaki, H., Malamy, J. E. and Benfey, P. N. (2000). Molecular analysis of SCARECROW function reveals a radial patterning mechanism common to root and shoot. *Development* **127**, 595-603.

Xu, J., Hofhuis, H., Heidstra, R., Sauer, M., Friml, J. and Scheres, B. (2006). A molecular framework for plant regeneration. *Science* **311**, 385-388.

DEVELOPMENT